O-414

J. Chem. Thermodynamics **1991,** 23, 653–665

Thermodynamic properties of ammonium haloplatinates

II. Heat capacity and thermodynamic functions of deuterated ammonium hexachloroplatinate $(ND_4)_2PtCl_6$ at temperatures from 5 K to 350 K

RON D. WEIR [a]

Department of Chemistry and Chemical Engineering, Royal Military College of Canada, Kingston, Ontario K7K 5L0, Canada

and EDGAR F. WESTRUM, JR.

Department of Chemistry, University of Michigan, Ann Arbor, MI 48109-1055, U.S.A.

(Received 16 November 1990)

The heat capacity of deuterated ammonium hexachloroplatinate $(ND_4)_2PtCl_6$ was measured at temperatures from 5 K to 350 K by adiabatic calorimetry. One λ-shaped anomaly, absent in the undeuterated salt, was found in the curve for heat capacity against temperature. This λ-shaped transition reaches its maximum $C_{p,m} \approx 59.3 \cdot R$ at (27.2 ± 0.05) K with $\Delta_{trs}S^{\circ}_{m} = (1.216 \pm 0.004) \cdot R$, characteristic of an order-disorder transition. Smoothed values of the standard thermodynamic quantities for pure $(ND_4)_2PtCl_6$ are tabulated at temperatures up to 350 K.

1. Introduction

The hexahalogenated metal salts in the family A_2MX_6 (A = an alkali metal, M = transition metal or polyvalent ion, and X = a halogen) normally crystallize at room temperature into the cubic antifluorite structure with space group Fm 3m or No. 225 O_h^5. Some compounds in this family experience structural phase transitions as the temperature is lowered, thereby changing into a phase of lower symmetry. However, other members of the family exhibit no sign of a transition.[1, 2] An empirical geometrical model[3] has been developed to account for the stability of those crystals whose phase transitions correspond to distortions of the unit cell. The model is based on the experimental finding that as the cation size increases and that

[a] To whom correspondence should be sent.

0021-9614/91/070653+13 $02.00/0

of halogen ligand decreases, the transition temperatures are shifted to lower values. It is also known that the transition temperatures depend on the d-electron configuration of the metal atom.[1] For some salts in this family, the transitions are accompanied by distortions of the cubic lattice but without a coupling to the octahedral rotations, while in other salts the transitions involve only small angle librations of the MX_6^{2-} octahedra.[1, 2, 4] For both K_2ReCl_6 and K_2OsCl_6, the transitions from cubic to tetragonal structures are displacive transitions caused by the softening of the rotary lattice modes.[5-7]

The replacement of the alkali metal by either NH_4^+ or ND_4^+ results in additional librational degrees of freedom. In addition in these $(NH_4)_2MX_6$ salts, the structural phase transition of the alkali-metal analogue is either lowered by the tetrahedral symmetry of the ammonium ion or suppressed entirely.[4] The presence of the polyatomic anion with the distribution of charge over the large area of atoms weakens the electrostatic attraction between any of these atoms and a hydrogen of an ammonium ion. This in turn leads to a low barrier for rotation of either NH_4^+ or ND_4^+.

The stable cubic phase[8] of undeuterated ammonium hexafluorosilicate $(NH_4)_2SiF_6$ exhibits no transition in its crystal structure below room temperature and heat-capacity measurements show no anomaly down to 25 K.[9] The barrier to rotation of the NH_4^+ is 1616 K based on heat capacities,[10] but 1107 K from n.m.r. results.[11] Heat-capacity measurements show no anomaly in the deuterated analogue $(ND_4)_2SiF_6$ over the temperature range $6 \leqslant T/K \leqslant 343$, and they yield a librational wavenumber for the ND_4^+ of 122 cm^{-1}.[12] Similarly the cubic $(NH_4)_2SnCl_6$ is also without a phase transition between 300 K and 20 K, but the barrier to NH_4^+ rotation is much lower at 740 K to 600 K.[10, 11, 14-16] However, the deuterated salt $(ND_4)_2SnCl_6$ undergoes a transition around 244 K manifested as a λ-shaped anomaly in the heat capacity.[17] Whether its high-temperature cubic structure changes as the temperature is lowered below 244 K is not known, but the low-temperature structure is currently under study by Powell and Weir.

The barrier to NH_4^+ rotation in $(NH_4)_2PtCl_6$ is even lower at 342 K,[16] which has spawned work to determine the rotational potential of NH_4^+ in this compound[18, 19] and in related ammonium hexachlorides.[20] Recent heat-capacity measurements by adiabatic calorimetry show neither transitions nor anomalies from 6 K to 348 K,[21] making this salt an ideal candidate for examining rotational motion of the NH_4^+. A knowledge of the heat capacity of the deuterated analogue should also help in understanding the mechanism of molecular rotation of the ammonium ion. At 300 K, both salts have an antifluorite-like structure with space group Fm 3m (No. 225 O_h^5) and four formula units in the face-centred cell.[22, 23] Each ammonium ion is coordinated with 12 equivalent Cl^- atoms at the corners of the unit cell and the hydrogen atoms within the NH_4^+ or ND_4^+ point towards empty corners as shown in figure 1 of reference 21. Rotation of the NH_4^+ or ND_4^+ is indicated around both a twofold and a threefold axis. The absence of published heat-capacity measurements for $(ND_4)_2PtCl_6$ has led us to determine these at temperatures from 5 K to 350 K by adiabatic calorimetry as part of our programme of study involving ammonium salts.

2. Experimental

The sample of $(ND_4)_2PtCl_6$ was prepared from $(NH_4)_2PtCl_6$ which was supplied by the Aldrich Chemical Company as 99.999 mass per cent pure according to the Certificate of Analysis. No other elements were detected by spectrographic trace analysis at the detection level of mass fraction 1×10^{-6}. The Guinier-de Wolff diffraction pattern of the $(NH_4)_2PtCl_6$ was in perfect agreement with the standard pattern for this compound[21] and showed no traces of NH_4Cl. About 12 g was dissolved in 1300 cm^3 of D_2O (at least 99.8 moles per cent nuclidic purity) contained in a Pyrex beaker. To ensure complete dissolution, the yellow-orange mixture was warmed to 353 K. Upon recrystallization, a partially deuterated product was obtained. This procedure, carried out in a dry atmosphere, was repeated twice, whereupon the crystalline $(ND_4)_2PtCl_6$ product had a mass of 10.2 g. To remove most of the D_2O trapped as fluid inclusions in the crystals of $(ND_4)_2PtCl_6$ upon recrystallization, the salt was dried at atmospheric pressure within the dry box, where the sample was maintained at temperatures up to 313 K for 14 d with an infrared lamp. A t.g.a. was done on 10 mg to 20 mg samples removed at intervals.

The Guinier-de Wolff diffraction pattern of our sample was in agreement with the standard pattern for this compound: No. 7-218 as determined by the Joint Committee for Powder Diffraction Standards.[22] Its structure is face-centred cubic at room temperature with $a = (0.9856 \pm 0.0001)$ nm. Some scattering from a small amount of ND_4Cl impurity was noted.

As a check for D_2O trapped within our 'dried' sample of $(ND_4)_2PtCl_6$, the final t.g.a. was done on an 11 mg portion of the sample which was to be loaded subsequently into the calorimeter. On heating to 400 K, a mass loss of 0.18 per cent occurred, some of which was thought to be due to decomposed sample. The amount of D_2O present was expected to be lowered on loading the calorimeter, at which time the sample was vacuum pumped. A platinum resistance thermometer was used in the t.g.a. instrument to measure temperature and was calibrated at the ice point and the fixed points of the Curie transition in alumel at 422.5 K, in nickel at 631.2 K, and in Traflperm (97 mass per cent of Fe + 3 mass per cent of Si) at 1018.8 K. The estimated precisions were ± 2 K and $\pm 1 \times 10^{-6}$ g.

The molar heat capacity $C_{p,m}$ of the sample was measured at temperatures from 5 K to 350 K in the Mark XIII adiabatic cryostat, which is an upgraded version of the Mark II cryostat described previously.[24] A guard shield was incorporated to surround the adiabatic shield. A Leeds and Northrup capsule-type platinum resistance thermometer (laboratory designation A-5) was used for temperature measurements. The thermometer was calibrated at the U.S. National Bureau of Standards (N.B.S.) against the IPTS-48 (as revised in 1960)[25] for temperatures above 90 K, against the N.B.S. provisional scale from 10 K to 90 K, and by the technique of McCrackin and Chang[26] below 10 K. These calibrations are judged to reproduce thermodynamic temperatures to within 0.03 K, between 10 K and 90 K and within 0.04 K above 90 K.[27] Measurements of mass, current, potential difference, and time were based upon calibrations done at N.B.S. The acquisition of heat capacities was assisted[28, 29] by a computer programmed for a series of

determinations. During the drift periods, both the calorimeter temperature and its first and second derivatives of temperature with respect to time were recorded to establish the equilibrium temperatures of the calorimeter between the energy inputs. During energy inputs, the heater current and potential and the duration of the heating interval were obtained. Also recorded were the apparent heat capacity of the system including the calorimeter, heater, thermometer, and sample.

A gold-plated copper calorimeter (laboratory designation W-99) with four internal vertical vanes and a central entrant well for (heater + thermometer) was loaded with $(ND_4)_2PtCl_6$. After loading, the calorimeter was evacuated and pumping was continued for several hours to ensure that moisture was no longer released from the sample. After addition up to a pressure of about 2.4 kPa (at 300 K) of helium gas to the vessel to facilitate thermal equilibration, it was then sealed by means of an annealed gold gasket tightly pressed on to the stainless-steel knife edge of the calorimeter top with a screw closure about 5 mm in diameter.

Buoyancy corrections were calculated on the basis of a crystallographic density of $3.127\ g \cdot cm^{-3}$ derived from the unit cell edge of our sample. The mass of $(ND_4)_2PtCl_6$ amounted to 10.1819 g ($\triangleq$0.0225296 mol based on its molar mass of $451.9334\ g \cdot mol^{-1}$ from IUPAC 1983 atomic masses).

The thermal history of the $(ND_4)_2PtCl_6$ is represented by the following linear array. The arrows denote either cooling or heating, which correspond to the acquisition of heat-capacity results.

$$300\ K \xrightarrow{14\ h} 58\ K \xrightarrow{4\ h} 5\ K \xrightarrow[\text{Series I}]{3\ h} 20\ K \xrightarrow[\text{Series II}]{7\ h} 77\ K$$

$$\xrightarrow{4\ h} 15\ K \xrightarrow[\text{Series III}]{6\ h} 38\ K \xrightarrow{2\ h} 16\ K \xrightarrow[\text{Series IV}]{2\ h} 77\ K$$

$$\xrightarrow[\text{Series V}]{10\ h} 240\ K \xrightarrow[\text{Series VI}]{6\ h} 350\ K \xrightarrow{6\ h} 227\ K \xrightarrow[\text{Series VII}]{9\ h} 325\ K$$

$$\xrightarrow{10\ h} 225\ K \xrightarrow[\text{Series VIII}]{9\ h} 309\ K$$

3. Results and discussion

The experimental molar heat capacities for $(ND_4)_2PtCl_6$ are presented in table 1. Except for points in the region of the anomalies, the standard errors in our heat-capacity values decrease from about 1 per cent at 10 K to less than 0.15 per cent at temperatures above 30 K. The heat capacity of the sample represented about 0.45 to 0.60 of the measured total heat capacity away from the region of the anomalies.

Special care was taken with respect to particle size and thermal history of our $(ND_4)_2PtCl_6$ sample in view of the hysteresis in heat capacity found in other ammonium compounds, although no difficulty was experienced by us with $(NH_4)_2PtCl_6$.[21] However, reproducibilities of heat-capacity results for NH_4PF_6, $RbPF_6$, $(NH_4)_2SnCl_6$, K_2SnCl_6, and Rb_2SnCl_6 were all dependent on particle size,

TABLE 1. Experimental molar heat capacity of $(ND_4)_2PtCl_6$ ($M = 451.9334\ g \cdot mol^{-1}$; $R = 8.31451\ J \cdot K^{-1} \cdot mol^{-1}$)

T/K	$C_{p,m}/R$	T/K	$C_{p,m}/R$	T/K	$C_{p,m}/R$	T/K	$C_{p,m}/R$
Series I		25.42	6.415	203.74	30.34	296.34	33.39
5.60	0.0648	26.31	7.776	210.44	30.59	299.76	33.52
6.72	0.1160	26.93	22.13	217.14	30.93	303.19	33.65
8.43	0.2828	27.16	59.27	223.83	31.36	306.62	33.85
9.44	0.4025	27.29	51.02	230.51	31.84	310.04	33.99
10.45	0.5414	27.61	13.61	237.18	32.46	313.46	34.15
11.40	0.6905	28.37	6.403	Series VI		316.89	34.29
12.45	0.8698	29.40	6.210	$\Delta_{trs}H_m$ Detn.		320.31	34.42
13.54	1.097	30.38	6.441	256.80	32.36	323.74	34.56
14.63	1.340	31.54	6.762	269.84	32.83	Series VIII	
15.73	1.638	32.62	7.026	276.36	35.62	$\Delta_{trs}H_m$ Detn.	
16.92	2.005	33.64	7.286	283.07	33.44	226.24	31.52
18.19	2.443	34.60	7.572	289.85	33.27	229.74	31.76
19.49	2.890	35.52	7.793	296.52	33.38	233.87	32.08
Series II		36.31	8.016	303.15	33.72	238.01	32.52
19.15	2.758	37.07	8.223	309.77	33.96	242.15	33.02
20.56	3.202	37.78	8.449	316.39	34.29	246.26	33.66
21.90	3.683	Series IV		323.01	34.54	249.26	35.45
23.35	4.268	$\Delta_{trs}H_m$ Detn.		329.63	34.78	251.15	37.20
25.18	6.414	Series V		336.25	35.07	253.02	34.46
26.67	16.77	$\Delta_{trs}H_m$ Detn.		342.98	35.30	254.98	32.95
27.88	18.94	78.73	18.58	348.21	35.51	256.97	32.35
30.58	6.461	82.60	19.38	Series VII		258.97	32.38
33.31	7.205	86.69	20.19	$\Delta_{trs}H_m$ Detn.		260.98	32.41
34.99	7.634	91.02	20.90	229.15	31.72	262.98	32.43
36.71	8.123	95.58	21.65	232.52	31.95	264.97	32.56
38.43	8.611	100.37	22.34	235.95	32.19	266.95	32.62
40.35	9.097	105.34	23.03	239.38	32.67	268.93	32.75
42.46	9.688	110.39	23.70	242.78	33.10	270.91	32.93
44.57	10.26	115.45	24.28	246.20	33.62	272.90	33.14
46.69	10.86	120.53	24.83	249.56	35.80	274.87	33.37
48.91	11.43	125.61	25.33	252.94	34.70	276.79	35.83
51.28	12.14	130.95	25.86	255.83	32.37	278.70	34.35
53.78	12.73	136.55	26.38	258.70	32.38	280.63	33.59
56.39	13.46	142.15	26.87	262.14	32.44	284.54	33.33
59.14	14.16	147.77	27.33	265.54	32.56	286.49	33.27
62.03	14.85	153.39	27.71	268.94	32.76	288.82	33.26
65.06	15.63	159.28	28.12	272.37	33.07	291.54	33.29
68.26	16.36	165.45	28.49	275.75	34.92	294.24	33.34
71.62	17.12	171.62	28.79	279.14	34.23	296.93	33.42
75.16	17.83	177.78	29.14	282.61	33.45	299.63	33.53
Series III		183.95	29.46	286.08	33.29	302.30	33.64
18.86	2.681	190.37	29.75	289.50	33.27	304.99	33.63
22.47	3.839	197.05	30.09	292.92	33.30	307.67	33.92
24.12	4.776						

which in turn was affected by thermal history.[30, 31] A similar result was found in an n.m.r. study of KPF_6 and $RbPF_6$.[32] Our sample of $(ND_4)_2PtCl_6$ was ground to fine particles before it was loaded into the calorimeter and it was then cooled directly from 300 K to 5 K in 18 h when the measurements began. No differences are apparent between the heat-capacity values in our eight series of runs.

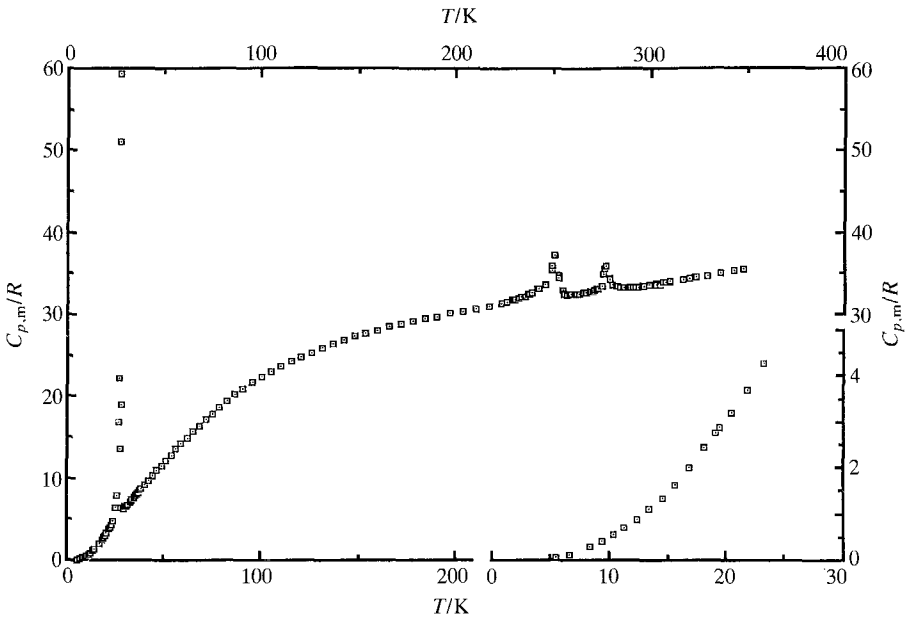

FIGURE 1. Experimental molar heat capacities at constant pressure plotted against temperature T for $(ND_4)_2PtCl_6$ containing impurities 0.07 mass per cent of D_2O and 0.25 mass per cent of ND_4Cl. The region below 25 K is enlarged in the lower right-hand corner.

A plot of experimental values of $C_{p,m}/R$ against T from 5.6 K to 348 K is shown in figure 1, where three anomalies are evident. One λ-shaped transition peaks with very high values around 27 K, and two smaller anomalies reach their maxima near 251 K and 277 K. By carrying out our heat-capacity measurements with sufficiently short heating intervals, the temperature where each heat capacity reaches the maximum was found to be (27.2 ± 0.05) K, (251.1 ± 0.1) K, and (276.8 ± 0.1) K for these three anomalies, respectively. Three passes were made through the region of the λ-shaped transition at 27 K (see the thermal history above: Series II, III, and IV), and reproducible heat capacities resulted. The details of the peak are shown in figure 2. The reproducibility of our measurements of the enthalpy and entropy changes through this region is presented in table 2.

The anomaly centred about 251.1 K and shown in detail in figure 3 corresponds to the phase transition in the ND_4Cl impurity, which reaches its peak in the pure salt around 250 K.[33, 34] The Guinier-de Wolff diffraction pattern confirmed the presence of ND_4Cl in our deuterated sample at 300 K. The impurity formed during the deuteration process, a phenomenon that we have occasionally experienced in other deuteration reactions. Three passes in four different series V to VIII were made through this anomaly to find the associated enthalpy. By interpolating the background heat-capacity curve from about 210 K to 260 K, the excess enthalpy and entropy associated with the anomaly were determined, which led to the calculation of the ND_4Cl impurity of 0.25 mass per cent.[33, 35] The experimental $C_{p,m}/R$ values

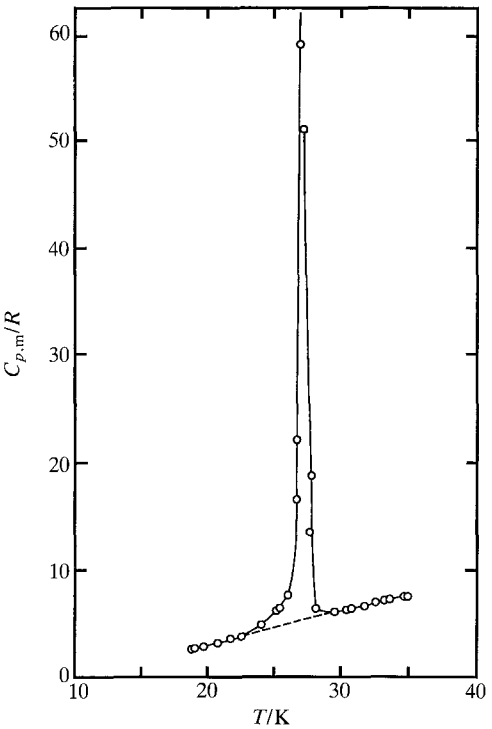

FIGURE 2. Experimental molar heat capacities $C_{p,m}$ at constant pressure plotted against temperature T through the region of the λ-shaped transition from 18 K to 35 K for $(ND_4)_2PtCl_6$; — — —, the lattice curve.

for the $(ND_4)_2PtCl_6$ sample given in table 1 were *not* adjusted for the ND_4Cl impurity.

The small peak at the highest temperature around 277 K corresponds to fusion of the saturated D_2O salt solution trapped as inclusions in the crystals of $(ND_4)_2PtCl_6$. The normal melting temperature of pure D_2O is about 276.27 K.[36] Three passes

TABLE 2. Summary of the thermophysical quantities through the λ-shaped transition at 27.2 K for $(ND_4)_2PtCl_6$ ($R = 8.31451\ J \cdot K^{-1} \cdot mol^{-1}$). T_1 and T_2 denote the beginning and ending temperatures, respectively, for three enthalpy determinations (Series IV) through the transition

T_1/K	T_2/K	$\frac{\Delta_{T_1}^{T_2} H_m^\circ}{R \cdot K}$	$\frac{\Delta_{22\,K}^{30\,K} H_m^\circ}{R \cdot K}$	$\frac{\Delta_{22\,K}^{30\,K} S_m^\circ}{R}$
21.505	33.793	101.5	73.67 ± 0.05	
Graphical integration			73.63 ± 0.05[a]	2.773 ± 0.002
Lattice contribution			40.69 ± 0.05[a]	1.557 ± 0.002
$\Delta_{trs} H_m^\circ/(R \cdot K)$:			32.98 ± 0.10	
$\Delta_{trs} S_m^\circ/R$:				1.216 ± 0.004

[a] Error due to the uncertainty in the position of the lattice-heat-capacity curve through the region of the anomaly.

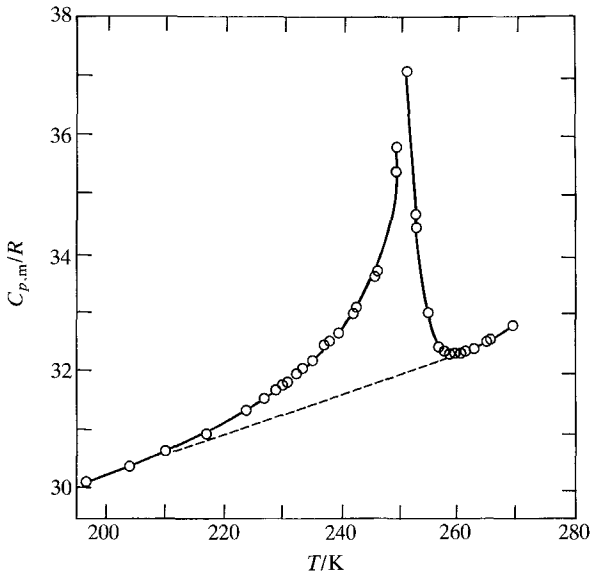

FIGURE 3. Experimental molar heat capacities $C_{p,m}$ at constant pressure plotted against temperature T through the region of the transition from 200 K to 270 K due to 0.25 mass per cent of ND_4Cl in $(ND_4)_2PtCl_6$; – – –, the lattice curve.

(Series VI to VIII) were made through this anomaly to determine the associated enthalpy. By interpolating the background heat-capacity curve from about 265 K to 290 K, the excess enthalpy of 2.487 $J \cdot mol^{-1}$ associated with the anomaly was determined, which led to the calculation of the D_2O impurity of 0.07 mass per cent. The experimental $C_{p,m}/R$ values for our $(ND_4)_2PtCl_6$ sample shown in table 1 were *not* adjusted for the impurity.

Integration of the smoothed values for experimental heat capacity and for the enthalpy and entropy increments through the anomalies yielded the thermodynamic functions. Values of $C_{p,m}/R$ and the derived functions are presented at selected temperatures in table 3. The corresponding values for the lattice curve beneath the anomalies, drawn by smooth interpolation, are given in parentheses. The heat capacities of $(ND_4)_2PtCl_6$ below 5 K were obtained by fitting our experimental values below 20 K to the limiting form of the Debye equation using a plot of $C_{p,m}/T^3$ against T^2 and extrapolating to $T \rightarrow 0$.

The values given in table 3 and plotted in figure 4 are for the pure salt and were obtained by correcting the smoothed experimental heat capacities for the 0.07 mass per cent of D_2O impurity as well as for the 0.25 mass per cent of ND_4Cl impurity noted above. The heat-capacity values of D_2O by Long and Kemp[36] were used, which lowered our $C_{p,m}$ values for $(ND_4)_2PtCl_6$ by about (0·1 to 0·2) per cent up to 200 K, by 0.23 per cent up to 270 K, and by about 0.50 per cent above 278 K. To correct our $C_{p,m}/R$ values for the 0.25 mass per cent ND_4Cl impurity, the heat-capacity values of NH_4Cl by Callanan, Weir, and Staveley[37] were taken since those for ND_4Cl are not tabulated by Stephenson *et al.*[35] Given the small amount of

TABLE 3. Standard molar thermodynamic functions for pure $(ND_4)_2PtCl_6$ ($M = 451.9334\ g \cdot mol^{-1}$, $p^\circ = 101.325\ kPa$, $R = 8.31451\ J \cdot K^{-1} \cdot mol^{-1}$, $\Phi_m^\circ \overset{def}{=} \Delta_0^T S_m^\circ - \Delta_0^T H_m^\circ / T$)

$\frac{T}{K}$	$\frac{C_{p,m}}{R}$	$\frac{\Delta_0^T S_m^\circ}{R}$	$\frac{\Delta_0^T H_m^\circ}{R \cdot K}$	$\frac{\Phi_m^\circ}{R}$	$\frac{T}{K}$	$\frac{C_{p,m}}{R}$	$\frac{\Delta_0^T S_m^\circ}{R}$	$\frac{\Delta_0^T H_m^\circ}{R \cdot K}$	$\frac{\Phi_m^\circ}{R}$
0	0	0	0	0	160	27.98	32.27	2679.5	15.52
5	(0.0420)	(0.0136)	(0.0526)	(0.0030)		(27.98)	(31.05)	(2646.5)	(14.51)
10	0.468	0.144	1.12	0.032	165	28.23	33.13	2820.0	16.04
15	1.443	0.498	5.66	0.121		(28.23)	(31.92)	(2787.1)	(15.02)
20	3.021	1.124	16.74	0.287	170	28.55	33.98	2961.9	16.56
21	3.346	1.279	19.92	0.331		(28.55)	(32.76)	(2929.0)	(15.53)
22	3.705	1.443	23.45	0.377	175	28.81	34.81	3105.3	17.07
23	4.160	1.618	27.38	0.427		(28.81)	(33.59)	(3072.4)	(16.04)
24	4.724	1.806	31.80	0.481	180	29.05	35.63	3250.0	17.57
	[a](4.449)	(1.799)	(31.64)	(0.481)		(29.05)	(34.41)	(3217.0)	(16.54)
25	5.500	2.016	36.95	0.538	185	29.30	36.43	3395.8	18.07
	(4.784)	(1.987)	(36.25)	(0.537)		(29.30)	(35.21)	(3362.9)	(17.03)
26	7.300	2.266	43.35	0.599	190	29.54	37.21	3542.9	18.56
	(5.113)	(2.181)	(41.20)	(0.597)		(29.54)	(35.99)	(3510.0)	(17.52)
27	25.80	2.732	55.77	0.666	195	29.77	37.98	3691.1	19.05
	(5.428)	(2.380)	(46.48)	(0.659)		(29.77)	(36.76)	(3658.2)	(18.00)
28	9.200	3.763	83.96	0.764	200	29.99	38.74	3840.5	19.53
	(5.737)	(2.583)	(52.08)	(0.724)		(29.99)	(37.52)	(3807.6)	(18.48)
29	6.197	4.004	90.84	0.872	205	30.14	39.48	3990.9	20.01
	(6.042)	(2.790)	(57.96)	(0.792)		(30.14)	(38.26)	(3957.9)	(18.96)
30	6.332	4.216	97.08	0.980	210	30.32	40.21	4142.0	20.48
	(6.332)	(3.000)	(64.14)	(0.862)		(30.32)	(38.99)	(4109.1)	(19.42)
35	7.654	5.290	132.0	1.518	215	30.49	40.92	4294.0	20.95
	(7.654)	(4.074)	(99.11)	(1.243)		(30.49)	(39.71)	(4261.1)	(19.89)
40	9.023	6.401	173.7	2.057	220	30.67	41.62	4446.9	21.41
	(9.023)	(5.185)	(140.8)	(1.665)		(30.67)	(40.41)	(4414.0)	(20.35)
45	10.41	7.543	222.3	2.603	225	30.85	42.32	4600.8	21.87
	(10.41)	(6.327)	(189.4)	(2.119)		(30.85)	(41.10)	(4567.7)	(20.80)
50	11.71	8.706	277.6	3.155	230	31.04	43.00	4755.4	22.32
	(11.71)	(7.490)	(244.7)	(2.597)		(31.04)	(41.78)	(4722.5)	(21.25)
55	13.04	9.884	339.5	3.712	235	31.23	43.67	4911.1	22.77
	(13.04)	(8.668)	(306.5)	(3.095)		(31.23)	(42.45)	(4878.1)	(21.69)
60	14.31	11.07	407.8	4.276	240	31.41	44.33	5067.6	23.21
	(14.31)	(9.857)	(374.9)	(3.609)		(31.41)	(43.11)	(5034.7)	(22.13)
65	15.55	12.27	482.4	4.845	245	31.58	44.97	5225.1	23.65
	(15.55)	(11.05)	(449.5)	(4.136)		(31.58)	(43.76)	(5192.2)	(22.57)
70	16.69	13.46	563.1	5.418	250	31.76	45.61	5383.4	24.08
	(16.69)	(12.25)	(530.2)	(4.672)		(31.76)	(44.40)	(5350.5)	(23.00)
75	17.75	14.65	649.2	5.994	255	31.93	46.24	5542.6	24.51
	(17.75)	(13.43)	(616.3)	(5.217)		(31.93)	(45.03)	(5509.7)	(23.42)
80	18.79	15.83	740.6	6.572	260	32.09	46.87	5702.7	24.93
	(18.79)	(14.61)	(707.6)	(5.767)		(32.09)	(45.65)	(5689.7)	(23.84)
85	19.73	17.00	836.9	7.151	265	32.24	47.48	5853.5	25.35
	(19.73)	(15.78)	(804.0)	(6.322)		(32.24)	(46.26)	(5830.6)	(24.26)
90	20.62	18.15	937.8	7.730	270	32.38	48.08	6025.0	25.77
	(20.62)	(16.93)	(904.8)	(6.880)		(32.38)	(46.87)	(5992.1)	(24.67)
95	21.44	19.29	1042.9	8.308	275	32.52	48.68	6187.3	26.18
	(21.44)	(18.07)	(1010.0)	(7.439)		(32.52)	(47.46)	(6154.3)	(25.08)
100	22.20	20.41	1152.0	8.885	280	32.66	49.27	6350.2	26.59
	(22.20)	(19.19)	(1118.1)	(7.999)		(32.66)	(48.05)	(6317.3)	(25.49)
105	22.88	21.51	1264.7	9.460	285	32.79	49.84	6513.8	26.99
	(22.88)	(20.29)	(1231.8)	(8.558)		(32.79)	(48.63)	(6480.9)	(25.89)

TABLE 3—*continued*

T/K	$C_{p,m}/R$	$\Delta_0^T S_m^\circ/R$	$\Delta_0^T H_m^\circ/R\cdot K$	Φ_m°/R	T/K	$C_{p,m}/R$	$\Delta_0^T S_m^\circ/R$	$\Delta_0^T H_m^\circ/R\cdot K$	Φ_m°/R
110	23.51	22.58	1380.7	10.03	290	32.93	50.42	6678.1	27.39
	(23.51)	(21.37)	(1347.8)	(9.116)		(32.93)	(49.20)	(6645.2)	(26.29)
115	24.09	23.64	1499.7	10.60	295	33.05	50.98	6843.0	27.78
	(24.09)	(22.43)	(1466.7)	(9.672)		(33.05)	(49.76)	(6810.1)	(26.68)
120	24.64	24.68	1621.5	11.17	300	33.17	51.54	7008.6	28.17
	(24.64)	(23.46)	(1588.5)	(10.23)		(33.17)	(50.32)	(6976.7)	(27.07)
125	25.15	25.70	1746.9	11.73	310	33.61	52.63	7342.5	28.95
	(25.15)	(24.48)	(1713.0)	(10.78)		(33.61)	(51.41)	(7309.5)	(27.84)
130	25.63	26.69	1872.8	12.28	320	34.05	53.71	7680.8	29.70
	(25.63)	(25.48)	(1839.9)	(11.32)		(34.05)	(52.49)	(7647.8)	(28.59)
135	26.09	27.67	2002.1	12.84	330	34.45	54.76	8023.2	30.45
	(26.09)	(26.45)	(1969.2)	(11.86)		(34.45)	(53.54)	(7990.3)	(29.33)
140	26.54	28.62	2133.6	13.38	340	34.84	55.79	8369.7	31.18
	(26.54)	(27.41)	(2100.8)	(12.40)		(34.84)	(54.58)	(8336.7)	(30.06)
145	26.94	29.56	2267.4	13.93	350	35.20	56.81	8719.8	31.89
	(26.94)	(28.35)	(2234.4)	(12.84)		(35.20)	(55.69)	(8686.9)	(30.77)
150	27.31	30.48	2403.0	14.46					
	(27.31)	(29.27)	(2370.0)	(13.47)	298.15	33.12	51.33	6947.3	28.03
155	27.66	31.38	2540.4	14.99					
	(27.66)	(30.17)	(2507.4)	(13.99)		±0.03	±0.05	±9.6	±0.03

[a] Quantities in parentheses represent the values taken on the lattice curve.

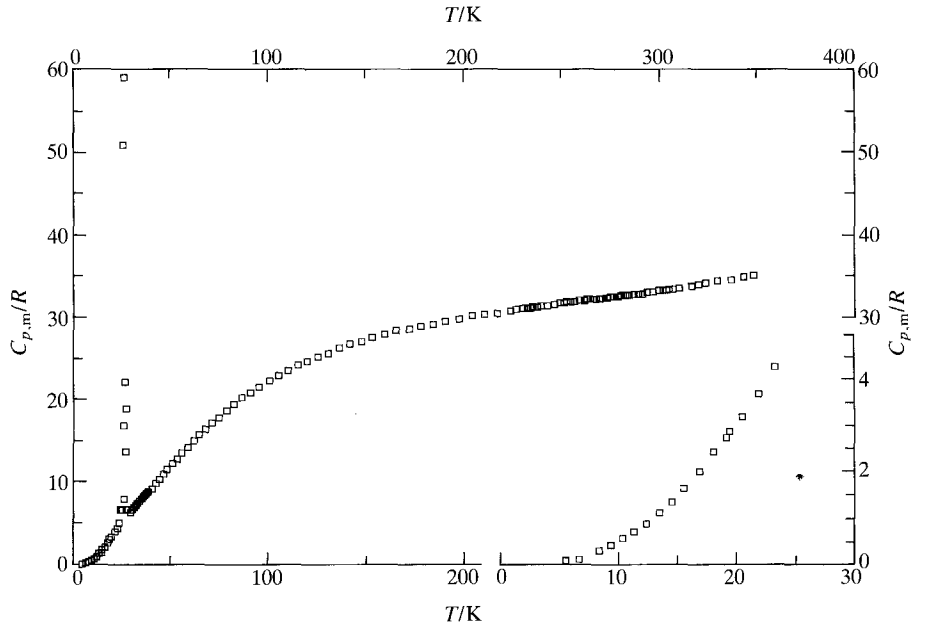

FIGURE 4. Experimental molar heat capacities $C_{p,m}$ at constant pressure plotted against temperature T for pure $(ND_4)_2PtCl_6$. The region below 25 K is enlarged in the lower right-hand corner.

impurity, the error introduced by this procedure is insignificant. There was a negligible correction to our $C_{p,m}$ values for $(ND_4)_2PtCl_6$ below 50 K, but they were lowered by (0.1 to 0.3) per cent up to 100 K, by 0.50 per cent up to 200 K, and by about 0.60 per cent up to 350 K.

The plot of $C_{p,m}/T^3$ against T^2 used to obtain heat capacities below 5 K is also useful for detecting any non-vibrational contributions to the heat capacity at low temperatures. The quantity measured calorimetrically is $C_{sat,m}$, which for these solids equals $C_{p,m}$. Moreover, the correction of $C_{p,m}$ to $C_{V,m}$, which is required for analysis of heat-capacity results, is negligible at these low temperatures. As a result, the heat capacity of our $(ND_4)_2PtCl_6$ insulator can be written as a power series.

$$C_{p,m} \approx C_{V,m} = aT^3 + bT^5 + cT^7 + \cdots. \tag{1}$$

The coefficients a, b, and c are directly related to the corresponding power series for the frequency spectrum at low frequencies.[38] Thus as $T \to 0$, the lattice heat capacity of the solid should become equal to that of an elastic continuum and can be approximated by the Debye T^3 law:

$$C_{V,m} = aT^3, \tag{2}$$

and

$$\Theta_D^C = (12\pi^4 Lk/5a)^{1/3}. \tag{3}$$

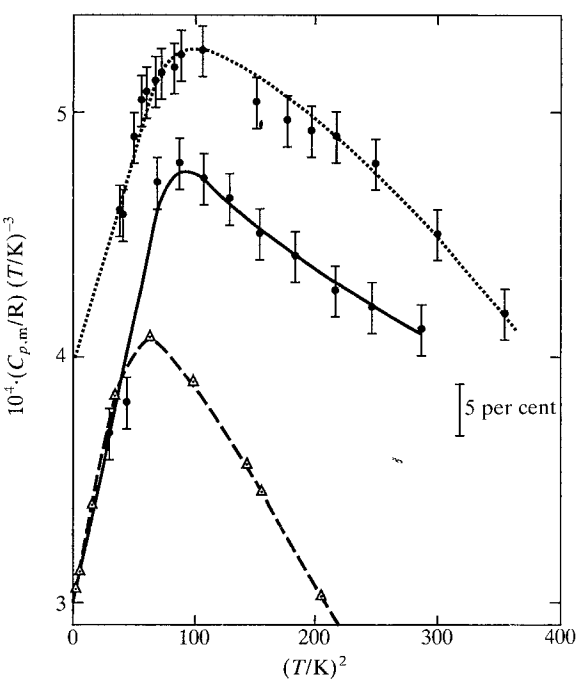

FIGURE 5. Experimental values of $C_{p,m}/(RT^3)$ plotted against T^2 for $(ND_4)_2PtCl_6$: ———, this work; ·····, $(NH_4)_2PtCl_2$ (reference 21); – – –, argon (references 38, 39). The vertical bars represent about 5 per cent in the $C_{p,m}$.

The Θ_D^C is the Debye characteristic temperature derived from heat capacities. The L and k are, respectively, Avogadro's and Boltzmann's constants. In figure 5 for the region $36 < (T^2/K^2) < 300$, the experimental heat capacities for $(ND_4)_2PtCl_6$ are no longer influenced by the λ-type transition near 27 K and follow a curve similar in shape to that for argon.[39,40] Hence only lattice vibrations make significant contributions to the heat capacity below 17 K. Extrapolation of the points below $T^2 = 30\,K^2$ in figure 5 to intersect the $T^2 = 0$ axis at a/R gives $10^4 \cdot a/R = (3.00 \pm 0.25)\,K^{-3}$ or $a \cdot 10^4 = (24.9 \pm 2.1)\,J \cdot K^{-1} \cdot mol^{-1}$. This yields from equation (3) $\Theta_D^C = (92.1 \pm 2.6)$ K and compares with 93.3 K for argon[39] and (83.7 ± 1.0) K for $(NH_4)_2PtCl_6$.[21]

The dearth of ancillary information about the spectroscopy, structure, and n.m.r. of the deuterated ammonium hexachloroplatinate handicaps a further interpretation of our heat capacities. The n.m.r. measurements[41] on $(NH_4)_2PtCl_6$, where no phase transitions occur, show that reorientation of the NH_4^+ dominates the relaxation between 55 K and 250 K and that $PtCl_6^-$ reorientation begins to contribute to the relaxation above 140 K. Whether this is also the case in $(ND_4)_2PtCl_6$ remains to be seen given the presence of the λ-shaped transition at about 27 K in this salt. The magnitude of the entropy change for the λ-shaped transition derived from our heat-capacity measurements suggests an order-disorder transition at 27.2 K with $\Delta_{trs}S_m^\circ = (1.216 \pm 0.004) \cdot R$ (compare ln 3 = 1.099, ln 4 = 1.386). The crystal structure needs to be determined near, but both above and below, 27.2 K.

We thank Dr R. D. Heyding for determining the crystal structure of our sample. One of us (RDW) thanks the Department of Defence (Canada) for financial support.

REFERENCES

1. Rössler, K.; Winter, J. *Chem. Phys. Lett.* **1977,** 46, 566.
2. Armstrong, R. L. *Phys. Rep.* **1980,** 57, 343.
3. Brown, I. D. *Can. J. Chem.* **1964,** 42, 2758.
4. Regelsberger, M.; Pelz, J. *Solid State Comm.* **1978,** 28, 783.
5. O'Leary, G. P.; Wheeler, R. G. *Phys. Rev.* **1970,** B1, 4409.
6. Lynn, J. W.; Patterson, H. H.; Shirane, G.; Wheeler, R. G. *Solid State Comm.* **1978,** 27, 859.
7. Mintz, D.; Armstrong, R. L.; Powell, B. M.; Buyers, W. J. L. *Phys. Rev.* **1979,** B19, 448.
8. Marignac, M. *Ann. Mines* **1857,** 12, 19.
9. Stephenson, C. C.; Wulff, C. A.; Lundell, O. R. *J. Chem. Phys.* **1964,** 40, 967.
10. Smith, D. *Chem. Phys. Lett.* **1974,** 25, 348.
11. Strange, J. H.; Terenzi, M. *J. Phys. Chem. Solids* **1972,** 33, 923.
12. Smith, D.; Weir, R. D.; Westrum, E. F., Jr. *J. Chem. Thermodynamics* **1990,** 22, 421.
13. Morphee, R. G. S.; Staveley, L. A. K.; Walters, S. T.; Wigley, D. L. *J. Phys. Chem. Solids* **1960,** 13, 132.
14. Svare, I. *J. Phys. C: Solid State Phys.* **1977,** 10, 4137.
15. Prager, M.; Press, W.; Alefield, B.; Hüller, A. *J. Chem. Phys.* **1977,** 67, 5126.
16. Svare, I.; Raaen, A. M.; Thorkildsen, G. *J. Phys. C: Solid State Phys.* **1978,** 11, 4069.
17. Callanan, J. E.; Weir, R. D.; Westrum, E. F., Jr. *J. Chem. Thermodynamics* **1990,** 22, 149.
18. Otnes, K.; Svare, I. *J. Phys C: Solid State Phys.* **1979,** 12, 3899.
19. Hoser, A.; Prandl, W.; Heger, G. *Proceedings ILL-IFF Workshop on Quantum Aspects of Molecular Motions in Solids.* Heidemann, A.; Magerl, A.; Prager, M.; Richter, D.; Springer, T.: editors. Springer: Berlin. **1986,** pp. 19–23.
20. Smith, D. *J. Chem. Phys.* **1985,** 82, 5133.
21. Weir, R. D.; Westrum, E. F., Jr. *J. Chem. Thermodynamics* **1990,** 22, 1097.

22. Swanson, H. E.; Gilfrich, N. T.; Ugrinic, G. M. *Natl. Bur. Stand. (U.S.) Circ. No. 539.* **1955,** 5, pp. 3–4.
23. Wyckoff, R. W. G. *Crystal Structures. Vol. 3.* Interscience: New York. **1965,** p. 342.
24. Westrum, E. F., Jr.; Furukawa, G. T.; McCullough, J. P. *Experimental Thermodynamics, Vol. I.* McCullough, J. P.; Scott, D. W.: editors. Butterworths: London. **1968,** p. 133.
25. Stimson, H. F. *J. Res. Natl. Bur. Stand.* **1961,** 65A, 139.
26. McCrackin, F. L.; Chang, S. S. *Rev. Sci. Instrum.* **1975,** 46, 550.
27. Chirico, R. D.; Westrum, E. F., Jr. *J. Chem. Thermodynamics* **1980,** 12, 311.
28. Westrum, E. F., Jr. *Proceedings NATO Advanced Study Institute on Thermochemistry, Viana do Castello, Portugal.* Ribeiro da Silva, M. A. V.: editor. Reidel: New York. **1984,** p. 745.
29. Andrews, J. T. S.; Norton, P. A.; Westrum, E. F., Jr. *J. Chem. Thermodynamics* **1978,** 10, 949..
30. Staveley, L. A. K.; Grey, N. R.; Layzell, M. J. *Z. Naturforsch.* **1963,** 18A, 148.
31. Morphee, R. G. S.; Staveley, L. A. K. *Nature* **1957,** 180, 1246.
32. Miller, G. R.; Gutowsky, H. S. *J. Chem. Phys.* **1963,** 39, 1983.
33. Parsonage, N. G.; Staveley, L. A. K. *Disorder in Crystals.* Clarendon: Oxford. **1978,** p. 312.
34. Levy, H. A.; Peterson, S. W. *Phys. Rev.* **1952,** 86, 766.
35. Stephenson, C. C.; Blue, R. W.; Stout, J. W. *J. Chem. Phys.* **1952,** 20, 1046.
36. Long, E. A.; Kemp, J. D. *J. Am. Chem. Soc.* **1936,** 58, 1829.
37. Callanan, J. E.; Weir, R. D.; Staveley, L. A. K. *Proc. Roy. Soc. London* **1980,** A372, 497.
38. Barron, T. H. K.; Berg, W. T.; Morrison, J. A. *Proc. Roy. Soc. London* **1957,** A242, 478.
39. Beaumont, R. H.; Chihara, H.; Morrison, J. A. *Proc. Phys. Soc. London* **1961,** 78, 1462.
40. Finegold, L.; Phillips, N. E. *Phys. Rev.* **1969,** 177, 1383.
41. Bonari, M.; Terenzi, M. *Chem. Phys. Lett.* **1974,** 27, 281.